

# INTERNATIONAL SOCIETY FOR SOIL MECHANICS AND GEOTECHNICAL ENGINEERING



*This paper was downloaded from the Online Library of the International Society for Soil Mechanics and Geotechnical Engineering (ISSMGE). The library is available here:*

<https://www.issmge.org/publications/online-library>

*This is an open-access database that archives thousands of papers published under the Auspices of the ISSMGE and maintained by the Innovation and Development Committee of ISSMGE.*

*The paper was published in the proceedings of the 11<sup>th</sup> Australia New Zealand Conference on Geomechanics and was edited by Prof. Guillermo Narsilio, Prof. Arul Arulrajah and Prof. Jayantha Kodikara. The conference was held in Melbourne, Australia, 15-18 July 2012.*

# SOME ASPECTS OF THE NUMERICAL MODELLING OF EPS GEOFOAM BEHAVIOUR

Le Ta<sup>1</sup>, Tim Hull<sup>1</sup> and Andrew Leventhal<sup>1</sup>

<sup>1</sup> GHD Geotechnics, 57-63 Herbert Street, Artarmon, NSW 2064, (Locked Bag 2727, St Leonards, NSW, 1590); Australia  
Corresponding author: le.ta@ghd.com

## ABSTRACT

Expanded polystyrene (EPS) geofoam is a highly non-linear material. Published research has shown that EPS geofoam under compression does not fail in the traditional sense observed in other materials, for example; soil, rock, concrete and steel. This paper presents the results of a small scale, non-standard laboratory investigation of the compressive behaviour of geofoam undertaken to help confirm the published stress strain relationship and to investigate the effect of significantly lowering the rate of strain/loading. A simple finite element box model was then analysed to study the impact of changing the Mohr Coulomb based input parameters (such as dilation angle) and the boundary conditions, in an attempt to better model the observed physical behaviour of the tests. The exercise was conducted for an engineering analysis modelling a slowly applied large strain upon geofoam.

*Keywords:* geofoam, EPS, stress strain behaviour, strain rate, numerical modelling.

## 1. INTRODUCTION

Geofoam is an extremely lightweight material made from expanded polystyrene, possessing a bulk density about 1% to 2% of the density of soil and rock. In the last 20 years, EPS geofoam has been commonly used in geotechnically related applications to replace conventional general fill. The primary application of geofoam has been to provide lightweight void fill for below highways and bridge approach embankments, embankment construction on low bearing capacity soft soils and the stabilisation of failed slopes. EPS geofoam is: easy to handle, thus speeding up construction; may possibly eliminate the need for preloading, surcharge and staged construction while leading to less settlement; and may reduce lateral stress on bridge approach abutments.

EPS geofoam may be considered to have more compressibility than other construction materials; however, standard tests are only of short duration and intended to inform modelling of small strain applications. Compression testing to investigate strain rate impact is thus required and Figure 1 shows the adopted test setup generally based upon standard procedures. A typical stress-strain curve of EPS geofoam derived from standard testing is shown in Figure 2 (NCHRP, 2004). It is noted that EPS geofoam does not fail in the sense associated with other traditional materials used in construction (such as soil, rock, concrete, metal and timber). The stress-strain relationship of EPS geofoam shown in Figure 2 can be divided into four zones as follows:

- Zone 1: Initial linear response. The initial region of linear stress-strain behaviour is below 1% to 1.5% strain.
- Zone 2: Yielding zone. The typical shape of this zone is similar to progressive yielding curves of other materials. The yield stress has been reported to increase with the density of the geofoam and the zone extends to strains of 10%.
- Zone 3: Linear and work hardening. After yielding in Zone 2, the stress-strain response of EPS geofoam is work hardening in nature. For this zone, the strain is from 10% to 35%.
- Zone 4: Non-linear and work hardening. The axial strain being between 35 to nearly 100%.

Zou and Leo (1998), Atmatzidis et al. (2001) and Zou (2001), between them, have carried out tests including unconfined compression and “undrained” triaxial tests to study EPS geofoam. The tests reveal an EPS Poisson’s Ratio of a small positive value during the initial stage of loading when strain was very small, which quickly reduced to zero. Poisson’s ratio then became a negative value at larger strains. The EPS geofoam specimen volume was contractive during “undrained” axial loading and the volume change was not accompanied by lateral volume expansion. At the end of the tests, the specimens showed a slight reduction in sample diameter.

While there is some information concerning the observed behaviour of geofoam, the authors found no information concerning translation of this data into the modelling of geofoam stiffness in a finite element modelling scenario involving slow strain rate driven “loading”.

**2. EPS GEOFOAM LABORATORY TESTS**

Uniaxial compression tests of polystyrene foam with density 0.02t/m<sup>3</sup> (Grade M) have been conducted by GHD Geotechnics. The general test arrangement is shown in Figure 1.

The first specimen of 65mm x 59mm x 59mm (length, breadth, vertical height dictated by available material) was subjected to rapid uniaxial compression load at a similar rate to previous tests (as suggested by NCHRP) such that the original specimen height reduced to 51%. The initial vertical stress applied on the geofoam to achieve this strain was 245kPa. This ad-hoc test was conducted to estimate the resistive stress generated in a strain-driven environment of approximately 50% strain. Load, time and foam dimension were monitored to study the geofoam response to the above initial vertical strain, followed by a strain relaxation and finally an unloading stage. The test was carried out over several days.

The second geofoam test was conducted upon a sample with dimensions of 52mm x 59mm x 59mm. The specimen was tested by increasing the vertical strain with time. The second test was carried out at a much slower displacement rate of an average 0.4mm/hour and over an extended period. Full results of the second compression test and, for clarity only the relaxation stage of the first test are given in Figure 2, together with a published stress-strain curve.



Figure 1: Polystyrene uniaxial test setup showing 50% strained position.

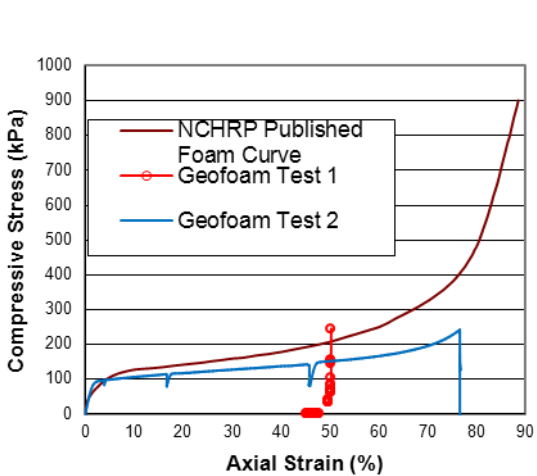


Figure 2: Geofoam compressive stress versus strain.

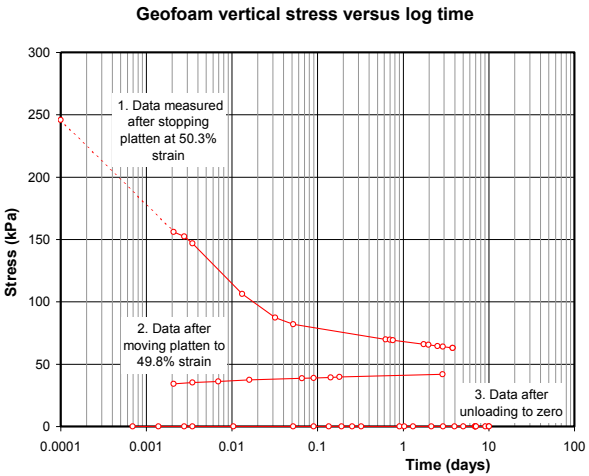


Figure 3: Test 1 compressive stress versus time.

Figure 3 shows the results of Test 1 and it may be seen that there is a bi-linear stress relaxation versus log time response. The first, steeper slope of relaxation of axial stress with time was observed for the first hour. Then a second, flatter slope stress relaxation occurred between 1 hour and 4 days and the stress was then possibly trending to a constant value after that. The observed stress relaxation at 50.3% strain may possibly be explained by air trapped in the EPS geofoam structure having escaped/seeped out slowly from the EPS specimen.

After a small movement of the platen upwards to achieve an unload to 34kPa, the sample height rebound was from the 29.5mm to 29.6mm (to 49.8% strain) and the axial stress eventually increased to 42kPa. The breadth reduced from 58mm to 57mm while the sample length remained at 63mm. Immediately after the specimen was unloaded, after nearly 7 days in the test rig, the height increased, rebounding from 29.6mm to 30.9mm, and the sample breadth also increased to 58mm, while the sample length was unchanged at 63 mm. The sample height then gradually increased from 30.9 mm to 32.36 mm during the elapsed time between 181 to 355 hours. Both the sample length and breadth were unchanged during this zero-load time.

Test 2 was carried out at a much slower strain rate than the initial loading stage of Test 1. This rate is representative of the slow movements associated with the impacts of strain-driven scenarios. The second test result in Figure 2 shows the EPS geofoam stress strain relationship had a very similar shape to the plot of NCHRP. However, the second geofoam test resulted in a smaller compression stress than the NCHRP results for the same strain level. The plot shows some downward spikes in the test result at axial strains of about 4, 17, 46 and 76 %. Those spikes have occurred at the times when the tests were paused and the axial strains remained constant. At each time the axial stress dropped down to a value less than 100kPa due to geofoam relaxation, before the test was reloaded. The axial stress then increased steeply back to the “virgin” compressive curve as the axial strain increased.

It is evident that strain rate has an impact on the magnitude of stress developed and that stress relaxation is significant. The behaviour in terms of minimal, to no, strain developing at right angles to the applied stress direction is important if the mechanical response of geofoam is to be modelled.

### 3. FINITE ELEMENT MODELS FOR A SIMPLE GEOFOAM BOX

As demonstrated above, geofoam is a highly non-linear material under compression loading. For an applied compressive stress greater than 100kPa, geofoam will behave in a non-linear sense and exhibit stress relaxation. From a FE modelling perspective, the physical behaviour of geofoam needs to be better represented at least up to the strains required by the subject engineering analysis.

To address this, a simple numerical box model was used to study the geofoam behaviour using the finite element program Phase<sup>2</sup> (RocScience, 1990), a two-dimensional elasto-plastic finite element program. The results suggest the accompanying lateral strains are small and therefore plane strain is a reasonable model. More work is needed to assess the possibility of anisotropy in the material.

In the study, the geofoam dilation angle and representative cohesion were varied. The plane strain models consisted of a box 50mm wide by 50mm high. The model boundary at the base was fixed in both x and y directions and the left, right boundaries were set to be free. The properties adopted for the base model of the finite element analyses, based on existing data, are: Unit weight of  $\gamma = 0.2\text{kN/m}^3$ , Young's modulus  $E = 5\text{MPa}$ , zero Poisson's ratio, tensile strength = cohesion strength of 40kPa, zero friction angle, residual cohesion of 40kPa and employing the “Body Force” option.

Five cases have been analysed with the geofoam modelled as:

Case 1: an elastic material.

Case 2: a plastic material with a zero dilation angle. This is the base case model.

Case 3: As per Case 2 but used negative 45° dilation angle.

Case 4: Case 3 but used geofoam cohesion and tensile strength set to 75kPa.

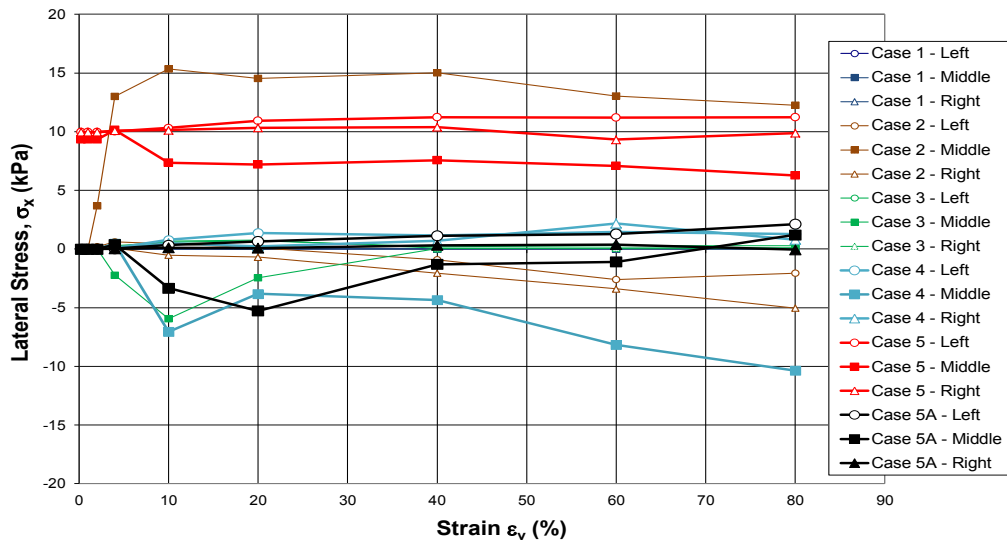
Case 5: As per Case 4 but the base was specified to be a smooth boundary. Furthermore, the side boundaries were loaded by a 10kPa lateral pressure to simulate a confining pressure.

Nine vertical displacement increments of 0.1, 0.5, 1, 2, 5, 10, 20, 30 and 40 mm were applied to the top surface boundary. The displacements were adopted to be equal to the percentage of vertical compressive strains to the geofoam box of 0.2, 1, 2, 4, 10, 20, 40, 60 and 80%, respectively.

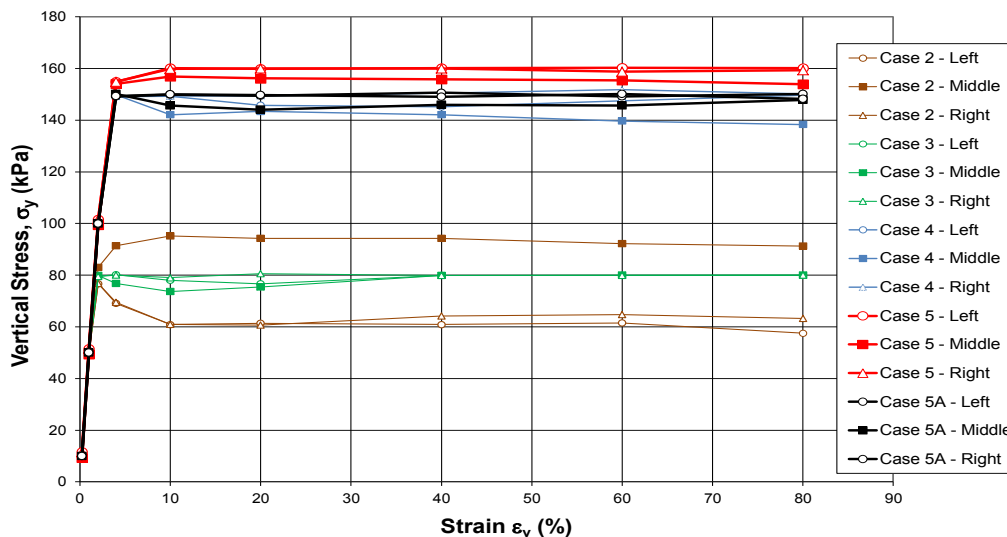
#### 4. FINITE ELEMENT RESULTS

Three selected locations near the extreme left, middle and extreme right at the mid-height have been adopted for the output results. As expected the left and right present more-or-less identical behaviour.

Plots of the lateral and vertical stress versus vertical strain are shown in Figures 4a and 4b. Note that for clarity the plots do not include the linear response of the elastic model Case 1 results, because the elastic model predicts unrealistically high vertical stresses that mask the results of Cases 2 to 5. Figure 5 shows the predicted geofoam Poisson's ratio ( $\nu$ ) for different values of vertical axial strain. It is noted that Poisson's ratio is defined as the average ratio of lateral strain divided by vertical strain. Figure 6 shows the plot of average lateral strain estimated from the left and right selected locations versus the vertical strain.



(a) Lateral stress



(b) Vertical stress

Figure 4: (a) Lateral and (b) vertical stress versus vertical strain, elastic model results not shown.

Figure 4a shows the response in terms of lateral stress:

- The lateral stress at the three selected locations in the elastic model for Case 1 is zero, which is consistent with the nominated zero Poisson's ratio.
- Case 2 shows some small negative lateral stress up to -5kPa on each side for a vertical strain value greater than 60%. However, the selected middle location for Case 2 shows relatively large positive lateral stress of about 15kPa at 10% vertical strain, which then reduces slightly to 12.5kPa at 80% strain.
- Case 3 shows essentially zero lateral stress, except for the middle location where the lateral stress is negative and between -2kPa to -6kPa for the strain range between 4% to 20% and then increases to nominally zero at 80% strain.
- The side locations of Case 4 predict some small positive lateral stress up to 1kPa. The middle point for Case 4 predicts the most overall negative lateral stress of -10kPa at 80% strain.
- Case 5 side locations predict a relatively constant lateral stress of about 10kPa. The middle point of Case 5 predicts slightly less with an average about 7kPa lateral stress.

Figure 4b shows the response in terms of vertical stress:

- Case 1 results are linear and, as expected, predict a very high vertical stress value of 4000kPa at 80% vertical strain and have been removed for clarity.
- The vertical stress in Cases 2 to 5 increases linearly at the small vertical strain values between 0 to 4% and then each case approaches relatively constant values after 10% strain.

It is noted that the vertical stress predicted by Cases 2 to 5 does not reproduce the slight increase with vertical strain as shown in the physical geofoam behaviour presented by NCHRP and evident in the Test 2 result. A strain hardening response has not been modelled in accordance with the restrictions imposed by the adopted Mohr Coulomb constitutive model.

It is also noted that the predicted maximum vertical stress in Cases 2 and 3, as would be expected from  $c = (\sigma_v - \sigma_h)/2$ , are equal to twice the cohesion plus the confining stress, that is for Cases 2 and 3,  $\sigma_v = 2c = 2 \times 40\text{kPa} = 80\text{kPa}$ . Similarly, the vertical stress for Case 4 is about 150kPa ( $2 \times 75\text{kPa}$ ) and Case 5 is 160kPa (i.e.  $\sigma_v = 2 \times 75\text{kPa} + 10\text{kPa}$ ).

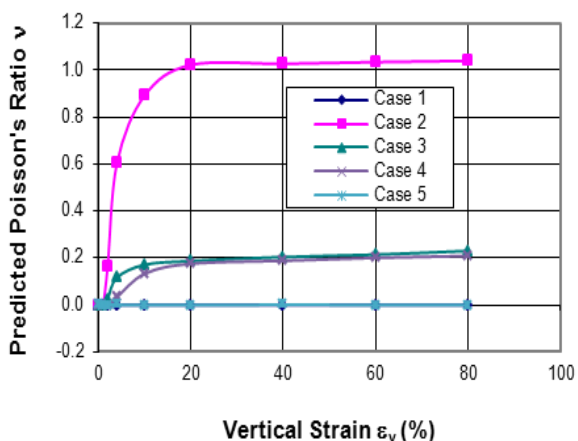


Figure 5: Estimated Poisson's ratio.

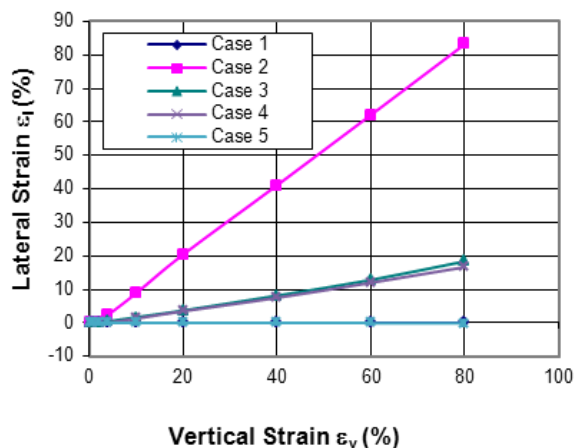


Figure 6: Estimated lateral strain.

Figure 5 plots the estimated Poisson's ratio versus vertical strain, where:

- The figure shows a zero Poisson's ratio for the elastic Case 1 and also the non-elastic Case 5.
- For the other cases, Poisson's ratio is predicted to be zero for small vertical strain values between 0.2 to 1%, and then increases with increasing strain level up to about 20% and becoming relatively constant after that.
- Cases 3 and 4 predict similar Poisson's ratio values however, Case 2 predicts the highest Poisson's ratio compared to other Cases. At 20% vertical strain level the predicted Poisson's ratio of Case 2 is 1.0 while Cases 3 and 4 are about 0.2 and Cases 1 and 5 are zero.

Figure 6 plots the geofoam lateral strain versus vertical strain. Wherein:

- The lateral strain predicted by Case 1 is about zero which is a consistent result for material with a zero Poisson's ratio, as shown in Figure 5.
- Cases 2 to 4 show that the lateral strain increases linearly with the vertical strain.
- Case 5 reproduces the required low (zero) lateral strain as observed in the tests.

Not surprisingly, the elastic, Case 1, shows excellent results for the lateral stress, lateral displacement and Poisson's ratio. However, Case 1 predicts very large compressive stress in comparison with the NCHRP stress-strain plot and other test results. The compressive stress predicted by Case 1 is unrealistic beyond low strain levels, that is, beyond the linear region of response.

Case 2 has predicted overall very poor results. This case has predicted the output Poisson's ratio greater than a unity for the vertical strain greater than 20%.

Cases 3 and 4 produce reasonable lateral stresses and a reasonable Poisson's ratio for the small vertical strain level. However, they predict lower vertical stress for a vertical strain greater than 10% in comparison with the observed stress-strain behaviour and for vertical strains greater than about 4%, these cases produce an erroneous Poisson's ratio, greater than zero.

Case 5 has overcome the Poisson' ratio error of Cases 3 and 4 by the correct nomination of the geofoam base roller boundary condition. While it is true that Case 5 still did not fully reproduce the strain hardening physical behaviour observed in geofoam, the general trends of the remaining behaviour are reasonably matched.

To confirm the commonly observed minimal impact from the application of the small lateral stress, Case 5 was reanalysed but without the 10kPa lateral confining pressure on the geofoam box. The results, which were essentially unchanged, are not shown in the above figures and provide a maximum vertical stress of 150kPa (i.e.  $\sigma_v = 2c = 2 \times 75\text{kPa}$ ).

#### 4. CONCLUSION

In summary, the commercially available values for properties of geofoam from "standard tests" were found to be inadequate for a project with long-duration and large strains imposed upon geofoam. In particular, the dilation angle that is required for Mohr Coulomb criterion based modelling using finite element software has no data. For a project that required this property, a dilation angle of  $-45^\circ$  is found to be appropriate and reflects the one-dimensional strength and "collapsing" zero lateral strain response observed in geofoam test results. With the adopted value, the box model reproduces the geofoam test results satisfactorily for the purpose of numerical modelling in Phase<sup>2</sup>.

The modelling of the behaviour of geofoam would be more satisfactorily treated by a large strain based software code, which is not the basis of Phase<sup>2</sup>, however for practical purposes the adoption of the properties determined from the study led to results adequate for engineering purposes.

#### REFERENCES

- Atmatzidis, D. K. and Missirlis, E. G. and Chryssikos DA., (2001). An investigation of EPS Geofoam behaviour in compression, EPS Geofoam 2001 – 3<sup>rd</sup> International Conference, Dec 10-12, 2001, Salt Lake City, Utah, USE.
- Stark, T., Arellano, D., Horvath, J. and Leshchinsky, D. (2004). Geofoam applications in the design and construction of highway embankments, prepared for National Cooperative Highway Research Program (NCHRP) Web Document 65 (Project 24-11), July 2004.
- RocScience, (1990-2011). Finite element program Phase<sup>2</sup>, RocScience Inc., Canada.
- Zou, Y. and Leo, C. J. (1998). Laboratory studies on engineering properties of expanded polystyrene (EPS) material for geotechnical applications, Proceedings of the 2<sup>nd</sup> International Conference on Ground Improvement Techniques, pp 581-588, 7-9 Oct, Singapore.
- Zou, Y. (2001). Behavior of the expanded polystyrene (EPS) geofoam on soft soil, PhD Thesis, School of Civic Engineering and Environment, The University of Western Sydney Nepean, Australia.